Simulation and Experimental Verification of Statistical Bias in Laser Doppler Anemometry including Non-Homogeneous Particle Density

W. Fuchs, H. Albrecht, H. Nobach
Electrical Engineering, University of Rostock, Germany
C. Tropea
INVENT GmbH, Erlangen-Tennenlohe, Germany
L.J.W. Graham
Dept. of Mechanical Eng., University of Queensland, Australia

ABSTRACT

The correlation between the measured velocity component and the instantaneous particle rate in laser anemometry leads to a statistical bias of most commonly used estimators. An additional bias may occur in non-homogeneously seeded flows if a correlation exists between the velocity and the particle density. These statistical bias effects are investigated using numerical simulations. Models for the particle arrival statistics are derived using autoregressive (AR) time series of the first order, generated for three velocity components with prescribed means, Reynolds stress tensor and time scales of the three normal stress tensor terms. The expected results obtained with commonly used processors and sampling techniques are investigated for various prescribed homogenous and inhomogeneous particle densities. The numerical results are compared to existing theoretical solutions and to some initial experimental results, obtained in an axisymmetric, co-flowing free jet. Some comparisons between one-dimensional and three-dimensional flowfields are also presented.

INTRODUCTION

The use of the laser Doppler anemometer (LDA) to measure flow velocities depends on the existence of small scattering particles in the flow which exhibit negligible slip velocity. Conventional application of the LDA technique assumes that the particle density is homogeneous throughout the flow and for these conditions numerous estimators for the statistical moments and the power spectrum of the flow velocity have been derived and analysed, including residence time weighting (Buchhave *et al.* 1979), sample and hold processors (Edwards and Jensen 1983, Adrian and Yao 1987) and controlled processors (Erdmann and Tropea 1984). The need for special estimators arises because the underlying process exhibits, in general, a non-zero correlation between the sample rate and the measured quantity. This *particle rate - velocity* correlation leads to the well documented velocity bias if simple arithmetic averaging is used as an estimator.

The correct choice of estimator may depend on numerous parameters, the most important being the statistics of the flowfield, the particle concentration and the functioning of the sampling and processing software and hardware (Edwards 1987). Two recent studies (Winter *et al.* 1991a, 1991b) have been particularly successful in identifying the most important time scale ratios and their influence on the error of controlled processors and sample-and-hold processors. These studies will also be used for comparison in the present work.

One major problem in the study of LDA estimators is that an experimental error evaluation is always difficult without a reference measurement of known accuracy. Thus, numerical simulations have often been used to verify or extend theoretical analysis. This paper also introduces a numerical simulation of a three-dimensional flowfield with seeding particles and a selectable processing and acquisition system. The simulation is based on concepts first introduced by Tropea (1987) in which autoregressive functions are used to generate primary velocity time series of known statistical properties. In a 'conveyor-belt' fashion, particles are then distributed in space and moved through the control volume according to the instantaneous velocity. Buchhave *et al.* (1990) also used this approach and extended it to three-dimensional flowfields. The present simulation improves the modelling presented by Buchhave (1990) and extends it to also include residence time modelling.

Non-homogeneous particle densities may also influence the correlation between velocity and particle rate and thus be an influencing factor on the accuracy of the chosen estimator. The simplest example is the free jet, in which the seeded jet air issues into non-seeded ambient air (Birch and Dodson 1988). Other sources of non-homogeneous particle densities include combustion, temperature variation or pressure variations, as pointed out by Asalor and Whitelaw (1975). Although this potential source of error has been recognized by numerous authors (Dibble *et al.* 1987, Durox and Baritaud 1987, Weckmann *et al.* 1986) little theoretical treatment has been attempted and empirical estimates of the measurement error are only very approximate. One exception is the circular jet investigated by Lehmann (1989), in which conditional seeding of the inner flow and of the entrained flow was used.

Therefore the numerical simulation was also designed to accept arbitrary correlations between the measured velocity component and the instantaneous particle density. Experiments in a co-flowing jet have been performed in which the seeding density of the outer and inner jet could be carefully controlled. The strategy is to verify the simulation model for selected conditions and then use the model to study further, arbitrary conditions.

The following section introduces the simulation model and program. The model is verified by comparison to various theoretical and known experimental results in section 3. A description of the experiments and a comparison between experimental results and numerical simulations is given in section 4. Section 5 presents a brief summary of the conclusions.

FLOW SIMULATION MODEL AND DATA PROCESSING

The simulation of LDA data from a 3D turbulent flowfield with known statistical properties is performed in a number of independent steps as represented diagrammatically in Fig. 1. Initially a velocity time series, or primary time series, is generated at regular and very closely spaced points in time. This is performed using a first order autoregressive model as described below. Second, the next particle distance from the control volume is generated according to the desired concentration model. In a conveyor-belt manner, the primary velocity series is integrated until the particle arrives in the control volume, yielding the arrival time. This is repeated for the next particle and so on, resulting in a secondary time series of particle velocities and arrival times. Since the velocity vector at the instant of particle arrival is known, a residence time can also be generated, knowing the measuring control volume (mcv) dimensions and assuming a random entrance position of the particle into the mcv. These two generation steps, i.e. primary and secondary time series are described in detail below.

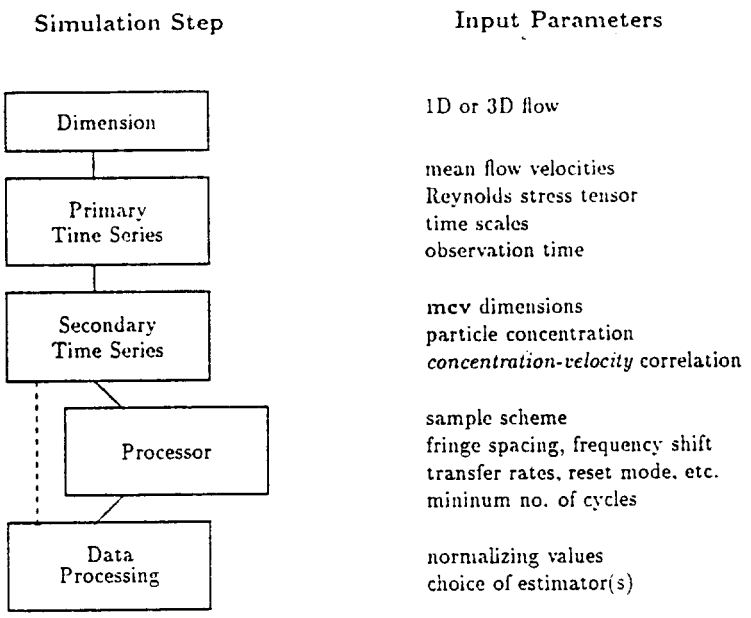

Figure 1: Schematic Representation of Simulation Program

Processing of the data then consists of prescribing a sample scheme, for example equidistant in time using the last valid particle (sample and hold), a controlled processor, a free-running processor, etc. Provision is made for specifying maximum data transfer rates, i.e. system dead times processor reset, etc. Note, that processors which perform multiple measurements per bursts can also be simulated since the Doppler frequency, the residence time and the frequency shift are all known quantities in the program. A minimum and optionally a maximum number of periods required for frequency estimation is always specified.

Finally, statistics according to the chosen sampling scheme and estimator are computed and compared with the known properties of the flow. Standard estimators are arrival time weighting, transit time weighting, sample and hold, simple arithmetic averaging and weighting according to the instantaneous measured velocity.. If it can be assumed that all particles are processed and only one frequency value per particle is used, the data processing can be performed directly on the secondary time series without including the processor step.

Fig. 1 indicates the various steps in the computer simulation. The data generated at each step can also be stored in files. Thus systematic parameter variations and their effect on a common simulated time series can easily be investigated.

Primary Time Series

In the following discussion the generation of a 3D velocity time series using a first order autoregressive (AR) model is described. A higher order AR model offers no improvement in the modelling of the turbulence spectrum and furthermore higher order models can no longer be expressed in closed form for programming.

First order AR series are used to generate three independent series (Box and Jenkins 1976)

$$\vec{z_t} = \begin{bmatrix} z_{x_t} \\ z_{y_t} \\ z_{z_t} \end{bmatrix} = \begin{bmatrix} \phi_x z_{x_{t-1}} + a_{x_t} \\ \phi_y z_{y_{t-1}} + a_{y_t} \\ \phi_z z_{z_{t-1}} + a_{z_t} \end{bmatrix} \tag{1}$$

with

$$a_{i_t} = \sqrt{1-\phi_i^2}\, x_{i_t} \tag{2}$$

where x_{i_t} are normally distributed random numbers with expectation zero and unity variance. The velocity vector is given by

$$\vec{v_t} = C\vec{z_t} + \overline{\vec{v}} \tag{3}$$

where $\overline{\vec{v}} = (\overline{v_x}, \overline{v_y}, \overline{v_z})$ is a prescribed mean vector and C is a symmetric covariance matrix. The covariance matrix (Reynolds stress tensor) of the series in Eq. 3 is given as

$$\Gamma_v = \begin{bmatrix} \gamma_{xx}, \gamma_{xy}, \gamma_{xz} \\ \gamma_{yx}, \gamma_{yy}, \gamma_{yz} \\ \gamma_{zx}, \gamma_{zy}, \gamma_{zz} \end{bmatrix} \tag{4}$$

with

$$\begin{aligned} \gamma_{xx} &= c_{xx}^2 + c_{xy}^2 + c_{xz}^2 \\ \gamma_{yy} &= c_{yx}^2 + c_{yy}^2 + c_{yz}^2 \\ \gamma_{zz} &= c_{zx}^2 + c_{zy}^2 + c_{zz}^2 \\ \gamma_{xy} = \gamma_{yx} &= c_{xx}c_{xy} + c_{xy}c_{yy} + c_{xz}c_{yz} \\ \gamma_{xz} = \gamma_{zx} &= c_{xx}c_{zx} + c_{xy}c_{zy} + c_{xz}c_{zz} \\ \gamma_{yz} = \gamma_{zy} &= c_{yx}c_{zx} + c_{yy}c_{zy} + c_{yz}c_{zz} \end{aligned} \tag{5}$$

The integral time scales of the series in Eq. 3, defined as the integral of the covariance coefficient, is given by

$$\Theta = \begin{bmatrix} \vartheta_{xx}, \vartheta_{xy}, \vartheta_{xz} \\ \vartheta_{yx}, \vartheta_{yy}, \vartheta_{yz} \\ \vartheta_{zx}, \vartheta_{zy}, \vartheta_{zz} \end{bmatrix} \tag{6}$$

with

$$\begin{aligned} \vartheta_{xx} &= \frac{1}{1-o_x}c_{xx}^2 + \frac{1}{1-o_y}c_{xy}^2 + \frac{1}{1-o_z}c_{xz}^2 \\ \vartheta_{yy} &= \frac{1}{1-o_x}c_{yx}^2 + \frac{1}{1-o_y}c_{yy}^2 + \frac{1}{1-o_z}c_{yz}^2 \\ \vartheta_{zz} &= \frac{1}{1-o_x}c_{zx}^2 + \frac{1}{1-o_y}c_{zy}^2 + \frac{1}{1-o_z}c_{zz}^2 \\ \vartheta_{xy} = \vartheta_{yx} &= \frac{1}{1-o_x}c_{xx}c_{yx} + \frac{1}{1-o_y}c_{xy}c_{yy} + \frac{1}{1-o_z}c_{xz}c_{yz} \\ \vartheta_{xz} = \vartheta_{zx} &= \frac{1}{1-o_x}c_{xx}c_{zx} + \frac{1}{1-o_y}c_{xy}c_{zy} + \frac{1}{1-o_z}c_{xz}c_{zz} \\ \vartheta_{yz} = \vartheta_{zy} &= \frac{1}{1-o_x}c_{yx}c_{zx} + \frac{1}{1-o_y}c_{yy}c_{zy} + \frac{1}{1-o_z}c_{yz}c_{zz} \end{aligned} \tag{7}$$

To summarize, the mean velocity vector, the Reynolds stress tensor (Eq. 4) and $\vartheta_{xx}, \vartheta_{yy}, \vartheta_{zz}$ are prescribed. The covariance matrix C is obtained by solving Eq. 5 iteratively. Eqs. 7(a-c) are then used to obtain $1/(1-o_i)$, which are then substituted into Eq. 7(d-f) to yield $\vartheta_{xy}, \vartheta_{xz}, \vartheta_{yz}$. The AR coefficients o_i are then used in Eqns. 1 - 3 to obtain the velocity vector time series.

Secondary Time Series

The particle concentration is always expressed (and entered) in terms of particles per integral time scale (α) of the measured velocity component (v_x). The mean velocity ($\overline{v_x}$) is used to convert this user input into a spatial distribution, i.e. particles per unit length of fluid which passes through the control volume. An exponential distribution is used to compute the distance to the next particle and an integration of the 3D velocity vector determines the corresponding arrival time.

For non-homogeneous particle concentrations, the above procedure is modified to allow various correlations between velocity and particle concentration. In particular, the exponential parameter becomes correlated with the instantaneous velocity. At present, linear and step-like correlations have been forseen, as summarized in Fig. 2. For linear correlation functions the average data density $\overline{\alpha}$ and the correlation slope must be prescribed. For step-like correlation functions the average data density and one of α_{min}, α_{max} or $\Delta\alpha$ must be prescribed. Also the velocity at which the correlation step occurs must be given.

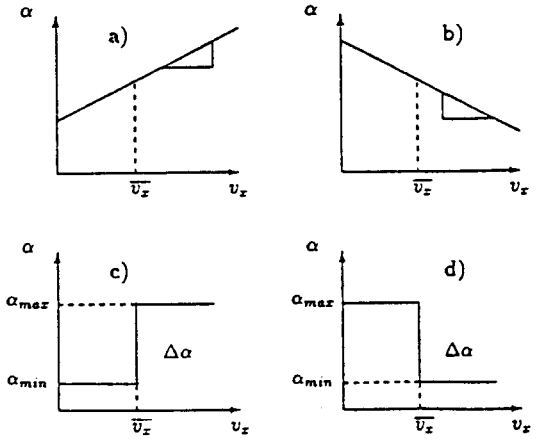

Figure 2: Correlation between particle concentration and velocity: a) linear positive; b) linear negative; c) step positive; d) step negative.

SIMULATION RESULTS

Simulation results were based on time series extending over 13,000 to 26,000 integral time scales ϑ_{xx}. In the following presentation only the expectation of the mean has been examined. The statistical bias has been expressed as a normalized error, which is the percent deviation from the true mean value (β) divided by the turbulence intensity squared (Tu^2).

$$\beta = \frac{\tilde{\overline{v_x}} - \overline{v_x}}{\overline{v_x}} \quad ; \quad Tu = \sqrt{\overline{v_x'^2}}/\overline{v_x} \tag{8}$$

$$\text{normalized error} = \beta/Tu^2 \tag{9}$$

The data density (N_D) is the number of velocity samples per integral time scale (ϑ_{xx}). The data rate has not been used explicitly in presenting these results. The time scales were chosen such that the primary time series had approximately 100 points per integral time scale. The major limiting factor in using the simulation program is the computation time. Using a 386-PC (33MHz) with co-processor, a 1D primary time series over 15,000 integral scales requires approximately 15 min computation time. The secondary time series requires about the same time again. Computations for 3D flows doubles the required time.

Homogeneous Seeding

In a first simulation three estimators of the mean velocity, an ensemble average (unweighted), arrival time weighting and transit time weighting have been computed as function of data density. In Fig. 3. results for a one-dimensional and a three-dimensional flow are presented. The turbulence intensity in the one-dimensional flow is 26%. In the three-dimensional flow all three normal stresses are 26% of $\overline{v_x}$, and $\overline{v_y}$ and $\overline{v_z}$ are set ot zero. Also the cross-correlation terms are equal to zero.

As expected, the free-running processor with ensemble averaging yields a constant normalized error of unity, independent of data density. This error reduces slightly for a three-dimensional flow, since the instantaneous particle rate is no longer solely determined by the measured velocity component, i.e. the v_y and v_z velocity components sometimes influence the particle rate. The arrival time weighting yields valid results only for data densities exceeding approximately $N_D = 10$. The transit time weighting is appropriate for both flows, showing some overcompensation in the case of a 3D flowfield.

In Fig. 4 two three-dimensional flowfields have been generated, the first one again with 26% turbulence and the second with 35% turbulence. At 35% turbulence first occurances of reverse flow are to be expected, thus the expected bias should decrease marginally for the ensemble mean. This is shown to be the case in Fig. 4. Otherwise the arrival time and transit time results are largely unaffected by turbulence level.

The statistical bias of the ensemble mean is also expected to decrease if the velocity component being measured is not the velocity component primarily responsible for the transport of particles through the measuring volume. A simulation experiment was therefore performed in which the velocity component perpendicular to the measured component was increased from zero mean to fourfold the measured mean. A three-dimensional simulation with a turbulence level of 26% based on the measured velocity component was used. Fig. 5 indicates that the ensemble and arrival time estimators yield better results since the underlying *measured velocity - particle rate* correlation has been reduced. The transit time weighted results are less affected, but do increase marginally, showing a small positive bias rather than a negative bias.

The above results indicate that the simulations yield trends agreeing with present understanding of the statistical bias of LDA mean estimators. In Fig. 6 one-dimensional simulations have been compared with experimental results from Winter et. al (1991a). Two estimators have been examined, the sample and hold, i.e. weighting with the arrival time to the *next* particle, and a controlled processor. The controlled processor arose due to a limited data transfer rate of 10 kHz. Therefore the bias begins to reduce at a data density of approximately $N_D = 1.6$ (ϑ_{xx} = 2.3ms) as predicted by Erdmann and Tropea (1984). These results also confirm those of Winter *et al.*(1991a), that a one-dimensional model is adequate for turbulence levels of 26%.

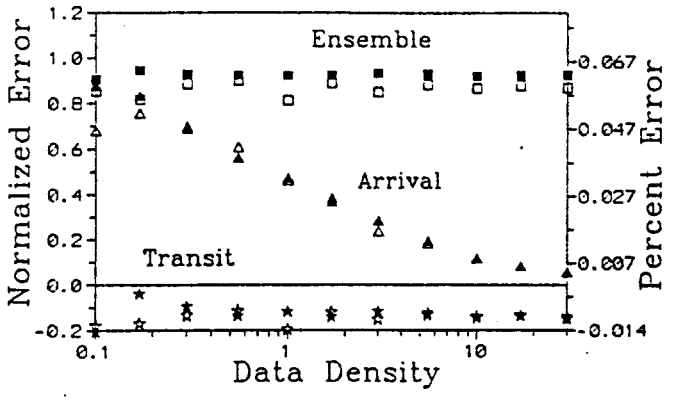

Figure 3: Bias magnitude as a function of data density (Tu = 26%): open symbols - 1D simulation; solid symbols - 3D simulation.

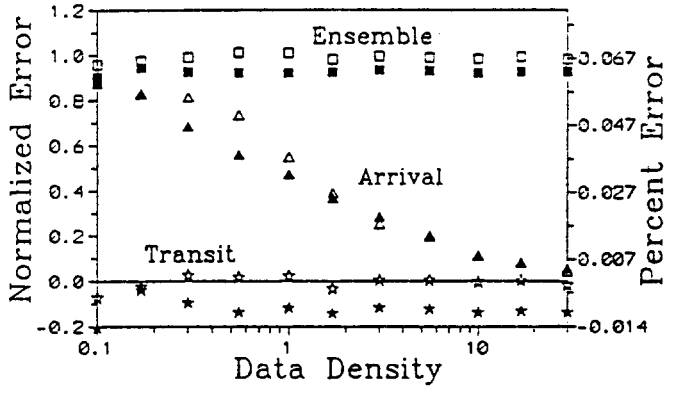

Figure 4: Bias magnitude as a function of data density using 3D simulation: open symbols - Tu = 35%; solid symbols - Tu = 26%.

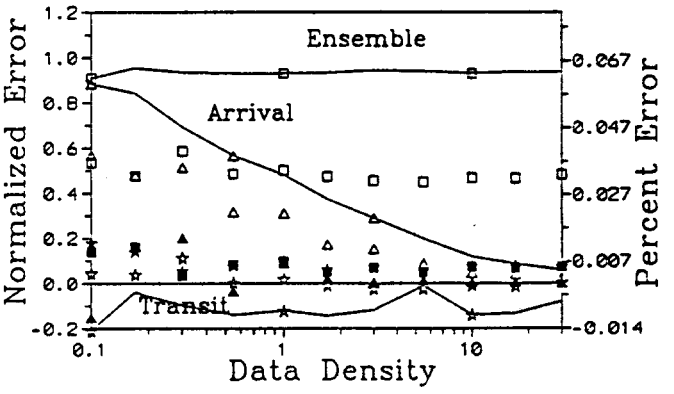

Figure 5: Bias magnitude as a function of data density (Tu = 26%): lines - $v_y = 0$; open symbols - $v_y = v_x$; solid symbols - $v_y = 4v_x$.

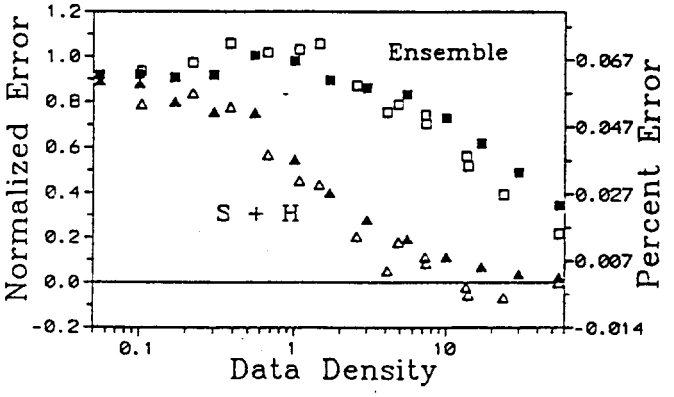

Figure 6: Comparison of simulated bias magnitude with experiments from Winter *et al.*(1991b): open symbols - experiments; solid symbols - simulation

Finally, in Fig. 7 the experimental results of Winter *et al.* (1991a) using a controlled processor have been compared with equivalent simulations, again at a turbulence level of 26%. Agreement is good for all values of the control period (ϑ_s) used.

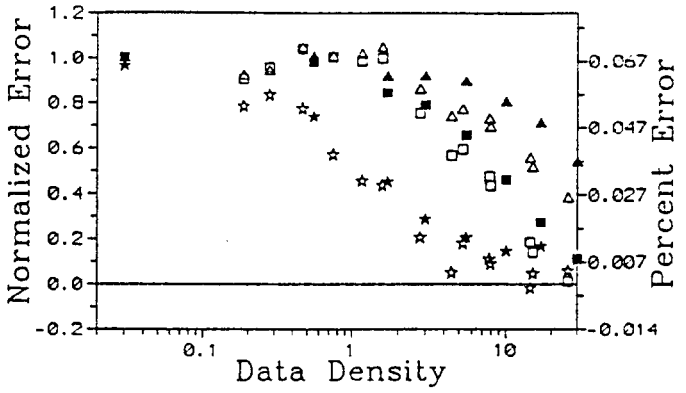

Figure 7: Comparison of simulated bias magnitude with experiments from Winter *et al.* (1991b): open symbols - experiments; solid symbols - simulation; △ - $\vartheta_s/\vartheta_{xx}$ = 0.043; □ - $\vartheta_s/\vartheta_{xx}$ =0.17; ⋆ - $\vartheta_s/\vartheta_{xx}$ =10.

Non-homogeneous Seeding

For simplicity the results presented below have been restricted to cases of linear correlations between velocity and particle density. The slope of the linear correlation is referenced to the case of homogenous seeding, i.e. a one-to-one correlation and is expressed by the coefficient

$$m_c = \frac{\partial \alpha}{\partial v_x} \cdot \frac{\overline{v_x}}{N_D} \qquad (10)$$

where α is the particle concentration in terms of particles per integral time scale (Fig. 2) and v_x is the measured velocity component. Therefore m_c = 0 for homogeneous seeding and m_c = 1 for a *particle-velocity* correlation leading to a statistical bias influence of the same order of magnitude as the velocity itself.

The behaviour of the previously examined estimators in non-homogeneously seeded flows is shown in Fig. 8 and 9, both valid for a one-dimensional flow with Tu = 26%. At low data densities the normalized bias of all estimators is increased by unity for the case of m_c = 1 (Fig. 8). As the data density increases, only the arrival time averaging tends towards a lower bias, reaching acceptable levels at N_D = 20. Note that the transit time weighting is *unaffected* by the data density.

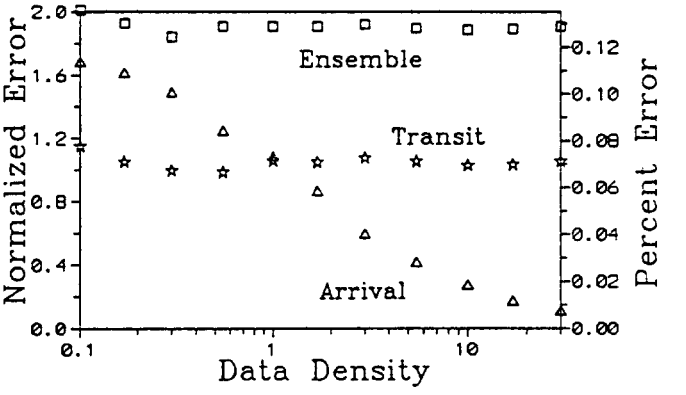

Figure 8: Bias magnitude for non-homogenous seeding: m_c = 1.

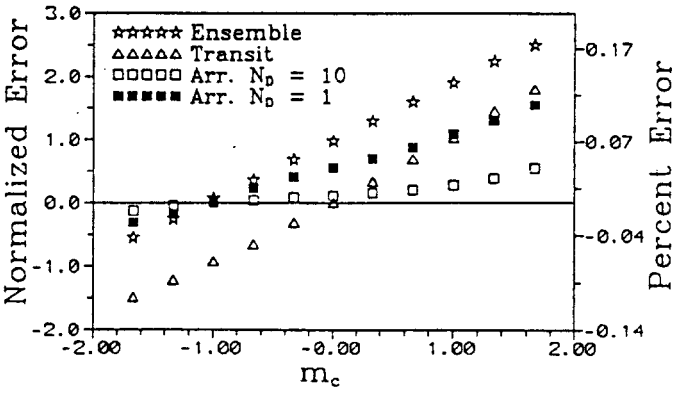

Figure 9: Bias magnitude for non-homogenous seeding.

Fig. 9 indicates that a negative *particle density - velocity* correlation leads to a decrease of the bias for ensemble averaging. The transit time weighting now overcompensates and leads to negative bias values. At higher data densities the arrival time weighting clearly yields the most accurate results. Results for controlled processors have however not yet been examined.

For non-homogenously seeded flowfields, little quantitative data on the effect of seeding density on mean estimators is available and for this reason an experiment was proposed and performed. A co-flowing jet was chosen in which the inner and outer flow could independently be controlled in velocity and seeding density. For these first experiments only the cases of seeding turned on or off in each of the two flows was used. As a reference, measurements were performed when both streams were seeded such that they had the same data density. This was checked by comparing the quotient - data rate $\dot{N}$ to mean velocity $\overline{v_x}$ - in the inner (x=10mm) and outer flow (x=-10mm) respectively. A sketch of the measurement region and the mean and RMS velocities are shown in Fig. 10.

Further detailed measurements were performed at a position y = 30mm, x = 1mm, marked on the profile of Fig. 10 with a dotted line. The turbulence of this position was 24% and the measured integral scale was 0.18ms. The integral scale was measured by taking data at a high, homogenous seeding density and performing and integrating a slot correlation. The velocity distribution at this position (transit time weighted) and at two neighbouring positions (x = 0mm, x = 2mm) are shown in Fig. 11, together with the change in integral scale. At homogenous seeding conditions the data density was approximately 0.1 particles per integral scale.

As a first step to compare simulations to experimental results, time series were generated for homogeneous seeding for the positions x = 0, 1 and 2 mm, such that the ensemble mean velocities at each point were in agreement with the experiments. The measured integral scales were used. Comparisons were then drawn for the arrival time and transit time weighting as shown in Fig. 12. The agreement shown here is good and therefore the time series are appropriate for investigating the cases of non-homogeneous seeding.

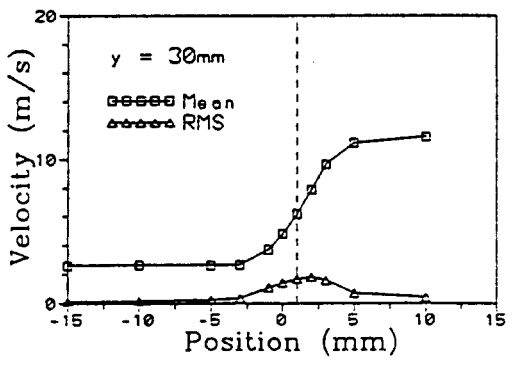

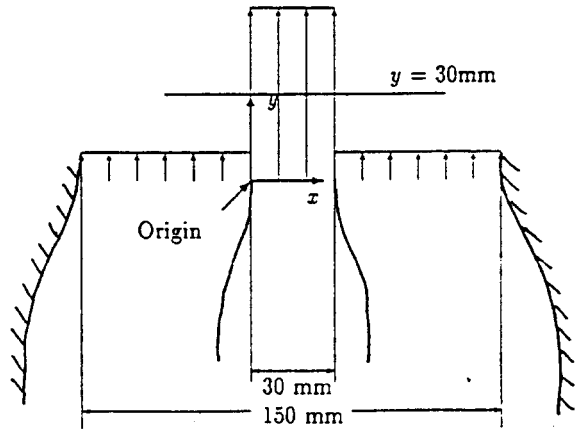

Figure 10: Schematic of co-flowing jet and velocity profile at downstream position of y = 30mm.

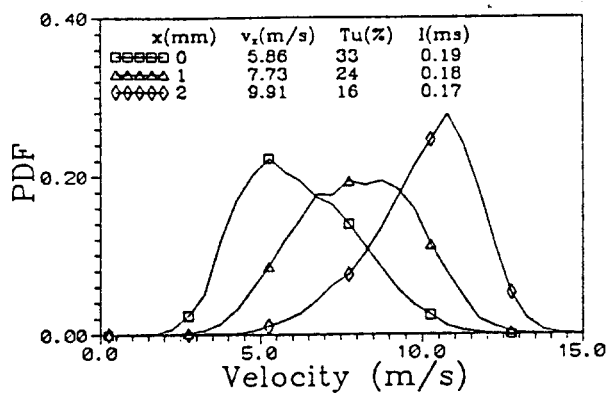

Figure 11: Velocity distributions at measurement point and at neighbouring points.

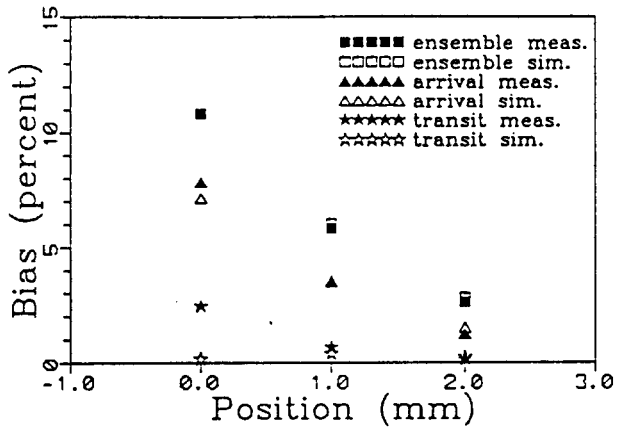

Figure 12: Comparison of predicted and measured bias of homogenously seeded flowfield: open symbols - simulation, solid symbols - measurements.

Simulations including the processor step were also performed, in which the parameters : number of fringes (93), shift frequency (0 MHz), operation mode (total burst), maximum data transfer rate (260 kHz for DOSTEK 1400A interface) and minimum number of cycles (8) were entered. There was however no deviation in the results from those using the secondary time series directly. Thus the processor was a true free-running processor and the processor step was left out of subsequent simulations.

For homogeneously seeded, 1D flows the data rate is linearly proportional to the velocity, i.e. $\dot{N}(v_x) = k_1 v_x$. for non-homogeneously seeded flows, in this case turning the inner or outer flow off, the data rate must be more generally related to the velocity, eq. $\dot{N} = f(v_x)$. For the ideal case, for instance when the outer flow seeding is turned off, the data rate in the mixing region takes the form

$$\begin{aligned} \dot{N} &= 0 \qquad v_x < v_o \\ &= k_1 v_x \qquad v_x > v_o \end{aligned} \tag{11}$$

In fact, this will never occur, since the mixing is not complete. It is important to understand that $\dot{N} = f(v_x)$ relates to the *instantaneous* velocity and not the *mean* velocity. Thus, even to measure the function f, a relatively high data density is required ($N_D > 20$), as is also the case to directly measure the relation between arrival time and instantaneous velocity! In the present experiment, values of N_D did not exceed 1.0, thus the function f could only be approximated by fitting the simulation to selected experimental results.

In Fig. 13 the function f is illustrated for homogeneous and non-homogeneous seeding (outer flow seeding turned off). It can be assumed that the shape of f lies between a linear positive and a step positive correlation.

For the present case, the parameter m_c in the simulation was therefore chosen to yield exact agreement to the measured ensemble and approximate agreement to the measured arrival/transit time weighted results. A summary of the results for inner and outer flow seeding is shown in Fig. 14a and 14b respectively. The chosen values for m_c are also included in this figure. The statistical bias has changed significantly compared to the results from a homogeneously seeded flow. Although previous results (Fig. 9) indicated that the arrival time weighted average should be consistently the most reliable estimator, the necessary data density of approximately $N_D = 10$ was not achieved in these experiments. Values of N_D varied between 0.3 and 1.0.

Finally, in a manner similar to Fig. 9, the measured bias is compared to the simulated bias (1D) in Fig. 15. For the experimental results shown in this figure the m_c value was that found iteratively while fitting the simulation results. Again, the agreement between simulation and experiment is very good.

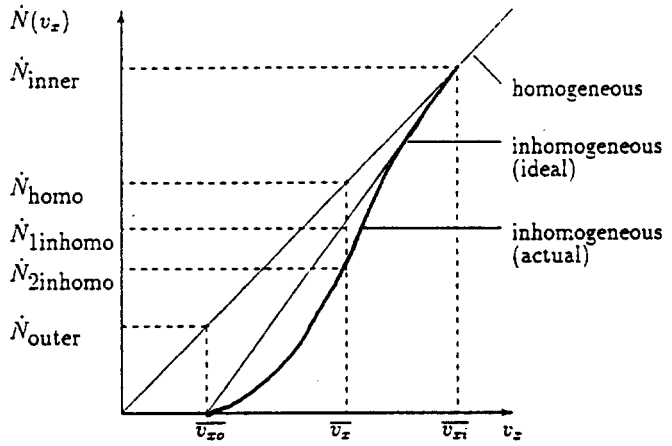

Figure 13: Schematic representation of relation between data rate and measured velocity for homogenous and non-homogenous seeding.

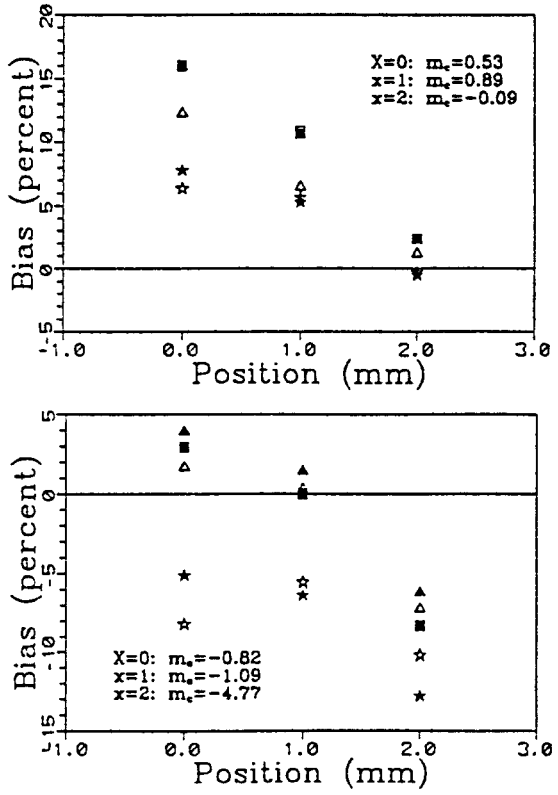

Figure 14: Comparison of predicted and measured bias a) inner flow seeding; b) outer flow seeding (symbols as in Fig. 12)

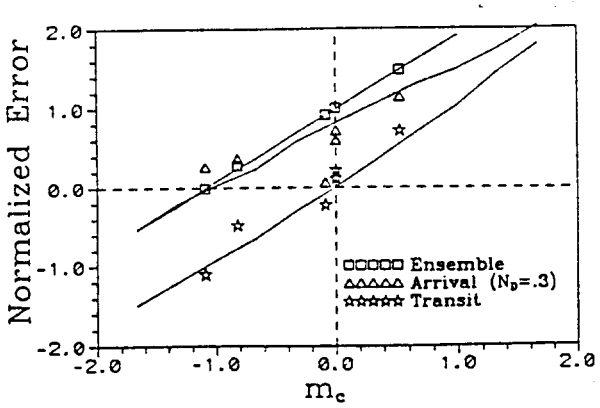

Figure 15: Comparison of predicted and measured bias as a function of parameter m_c: lines - predictions, symbols - experiments.

Conclusions

This work introduces a powerful simulation tool for investigating all aspects of statistical bias in laser anemometry. Results have been presented for mean velocity estimators, however extensions to variance or spectral estimators are straight-forward. The case of non-homogeneously seeded flow has been examined quantitatively and results indicate that correct measurements are possible using the arrival time weighting provided a minimum mean data density of $N_D > 10$ is achieved. Otherwise, the correct velocity measurement could be inferred by using the simulation program and fitting the parameter m_c to achieve agreement between ensemble, arrival and transit time weighted results.

Author JWG would like to acknowledge the CSIRO Postdoctoral Awards Scheme for supporting his trip to Europe. This work has been financially supported by the Volkswagen Foundation under contract I/66 487.

Bibliography

Adrian, R.J. and Yao, C.S. 1987 *Power Spectra of Fluid Velocities Measured by Laser Doppler Velocimetry* Exp. in Fluids 5, 17-28

Asalor, J.O. and Whitelaw, J.H. 1975 *The Influence of Combustion Induced Particle Concentration Variations in Laser- Doppler Anemometry* Proc. LDA-Symposium Copenhagen

Birch, A.D. and Dodson, M.G. 1980 *Some Aspects of Velocity Biasing in Turbulent Mixing Flows Resulting from Non-Uniform Seeding* Optica Acta 27, 3-8

Box, G.F.P. and Jenkins, G.M. 1976 Time Series Analysis: Forecasting and Control Holden Day, Oakland CA.

Buchhave, P., George, W.K.Jr. and Lumley, J. 1979 *The Measurement of Turbulence with the Laser Doppler Anemometer* Ann. Rev. of Fluid Mech. 11, Ann. Reviews Inc., Palo Alto, CA. 443-503

Buchhave, P., von Henon, H.-H. and Rasmussen, C.N. 1990 *LDA Bias: Comparison of Measurement Errors from Simulated and Measured Data* 5th Int. Symp. on Appl. of Laser Anemom. to Fluid Mechanics, Lisboa, LADOAN 29.3

Dibble, R.W., Hartmann, V. and Schefer, R.W. 1987 *Conditional Sampling of Velocity and Scalars in Turbulent Flames using Simultaneous LDV-Raman Scattering* Exp. in Fluids 5, 103-113

Durox, D. and Baritaud, T. 1987 *Statistical Bias in LDA Measurements* Dantec Info 4, Dantec Elektronik, Tonsbakken 16-18 DK-2740 Skovlunde, Denmark

Edwards, R.V. (Ed.) 1987 *Report of the Special Panel on Statisti- cal Particle Bias Problems in Laser Anemometry* ASME J. Fluids Engg. 109 pp. 89-93

Edwards, R.V. and Jensen, A.S. 1983 *Particle Sampling Statistics in Laser Anemometers: Sample-and-Hold Systems and Saturable Systems* J. Fluid Mech. 133, 397-411

Erdmann, J.C. and Tropea C. 1984 *Statistical Bias of the Velocity Distribution Function in Laser Anemometry* Laser Anemometry in Fluid Mechanics, Lisboa, LADOAN, 393-403

Lehmann, B. 1989 *Large-Eddy Interpretation of LDA Results Obtained by Conditional Seeding in a Circular Jet* Advances in Turbulence 2, Ed. H.-H. Fernholz and H.E. Fiedler, Springer-Verlag, Berlin

Tropea C. 1987 *Turbulence-induced Spectral Bias in Laser Anemometry* AIAA Journal 25, No. 2, 306-309

Weckmann, E.J., Sobiesiak, A., Tropea C., Brzustowski, T.A. 1986 *LDA Measurements in the Base Region of a Pool Fire* 3rd Int. Symp. on Appl. of Laser Anemom. to Fluid Mech. Lis- boa, LADOAN

Winter, A.R., Graham, L.J.W. and Bremhorst, K. 1991a *Velocity Bias Associated with Laser Doppler Anemometer Controlled Processors* ASME J. of Fluid Engg. 113, 250-255

Winter A.R., Graham, L.J.W. and Bremhorst, K. 1991b *Effects of Time Scales on Velocity Bias in LDA Measurements Using Sample and Hold Processing* Exp. in Fluids II, 147-152